Exceptionally Potent Anti–Tumor Bystander Activity of an scFv:sTRAIL Fusion Protein with Specificity for EGP2 Toward Target Antigen-Negative Tumor Cells[1]

Edwin Bremer, Douwe Samplonius, Bart-Jan Kroesen, Linda van Genne, Lou de Leij and Wijnand Helfrich

Groningen University Institute for Drug Exploration (GUIDE), Laboratory for Tumor Immunology, Section Medical Biology, Department of Pathology and Laboratory Medicine, University Hospital Groningen, Hanzeplein 1, Groningen 9713 GZ, The Netherlands

Abstract

Previously, we reported on the target cell–restricted fratricide apoptotic activity of scFvC54:sTRAIL, a fusion protein comprising human-soluble *t*umor necrosis factor–*r*elated *a*poptosis-*i*nducing *l*igand (TRAIL) genetically linked to the antibody fragment scFvC54 specific for the cell surface target antigen EGP2. In the present study, we report that the selective binding of scFvC54:sTRAIL to EGP2-positive target cells conveys an exceptionally potent pro–apoptotic effect toward neighboring tumor cells that are devoid of EGP2 expression (bystander cells). The anti–tumor bystander activity of scFvC54:sTRAIL was detectable at target-to-bystander cell ratios as low as 1:100. Treatment in the presence of EGP2-blocking or TRAIL-neutralizing antibody strongly inhibited apoptosis in both target and bystander tumor cells. In the absence of target cells, bystander cell apoptosis induction was abrogated. The bystander apoptosis activity of scFvC54:sTRAIL did not require internalization, enzymatic conversion, diffusion, or communication (gap junctional intracellular communication) between target and bystander cells. Furthermore, scFvC54:sTRAIL showed no detectable signs of innocent bystander activity toward freshly isolated blood cells. Further development of this new principle is warranted for approaches where cancer cells can escape from antibody-based therapy due to partial loss of target antigen expression.

Neoplasia (2004) **6**, 636–645

Keywords: scFv:sTRAIL, fusion protein, bystander, apoptosis, EGP2.

Introduction

In recent years, several antibody-based therapies that target tumor-associated membrane antigens have entered clinical trials with promising results [1–3]. However, curative treatment is frequently not achieved due to therapy-resistant recurrences emerging after initial rounds of seemingly successful treatment [4–6]. It has been shown that within one tumor mass, different stages of malignant progression and various oncogenic mutations can occur simultaneously, leading to the development of heterogeneous tumor cell phenotypes [7–12]. Heterogeneous and lost target antigen expression are likely to be responsible for many of the therapeutic failures observed in current antibody-based therapies [4–6].

Therefore, strategies have been developed to take advantage of the so-called "bystander effect," which aims to eliminate tumor cells with reduced or lost target antigen expression. The bystander effect is based on the principle that targeted tumor cells are not only eliminated, but are also exploited to convey the therapeutic effect toward neighboring tumor cells devoid of target antigen expression. Bystander effects have been described for several antibody-based therapeutic approaches [13,14] and, more recently, for gene therapy using FasL and *t*umor necrosis factor–*r*elated *a*poptosis-*i*nducing *l*igand (TRAIL)—two members of the tumor necrosis family of death-inducing ligands [15–18].

TRAIL is of particular interest for its tumor-restricted apoptosis-inducing capacity in a wide range of neoplastic cells while sparing normal tissues. TRAIL is expressed as a type II transmembrane protein (memTRAIL) [19,20] on a broad spectrum of tissues ranging from peripheral blood lymphocytes, spleen, and thymocytes to many solid organs, but is absent in the brain, liver, and testis.

A unique TRAIL receptor system has been uncovered in which the distinct receptors TRAIL-R1, TRAIL-R2, TRAIL-R3, TRAIL-R4, and osteoprotegerin (OPG) can differentially bind and interact with TRAIL. After ligation, TRAIL-R1 and TRAIL-R2 recruit the intracellular Fas-associated death domain

Abbreviations: TRAIL, tumor necrosis factor–related apoptosis-inducing ligand; scFv, single-chain fragment of variable regions; EGP2, epithelial glycoprotein 2; EGFP, enhanced green fluorescent protein; MFI, mean fluorescence intensity; FACS, fluorescence-activated cell sorting; PARP, poly(ADP-ribose) polymerase; HRP, horseradish peroxidase; ECL, enhanced chemoluminescence; GJIC, gap junctional intracellular communication

Address all correspondence to: Wijnand Helfrich, PhD, Laboratory for Tumor Immunology, Section Medical Biology, Department of Pathology and Laboratory Medicine, University Hospital Groningen, Building CMC VII, Room T2.228, Hanzeplein 1, Groningen 9713 GZ, The Netherlands. E-mail: w.helfrich@med.rug.nl

[1]This work was supported by a grant from the Dutch Cancer Society (project grant RUG 2002-2668) and by a grant from the Dutch Brain Foundation (project grant no. 10F02.30).

Received 18 March 2004; Revised 28 April 2004; Accepted 28 April 2004.

DOI 10.1593/neo.04229

(FADD) adapter protein and the initiator caspase-8 or caspase-10, thereby forming the death-inducing signaling complex (DISC) [21–28]. Assembly of the DISC results in activation of caspase-8 or caspase-10, which subsequently cleaves and activates effector caspases such as caspase-3, caspase-6, and caspase-7, leading to poly(ADP-ribose) polymerase (PARP) cleavage and, ultimately, apoptotic cell death. TRAIL-R3, TRAIL-R4, and OPG lack (functional) death domains and, after ligation, do not induce apoptosis.

TRAIL-R1 and TRAIL-R2 have a broad and partly overlapping pattern of expression, suggesting that they may serve as an alternate or "backup" system, allowing the immune system to control aberrant cells even if one of the receptors has failed. Recently, it was shown that TRAIL-R1 and TRAIL-R2 have rather distinct cross-linking requirements for the initiation of apoptosis [29]. Both recombinant soluble TRAIL (sTRAIL), consisting of the extracellular domain of TRAIL, and memTRAIL can efficiently activate TRAIL-R1 even at low concentrations, whereas TRAIL-R2 can only be activated by memTRAIL or sTRAIL that is secondarily cross-linked by antibodies.

To date, various forms of recombinant sTRAIL have been generated, of which potent anti–tumor activity has been demonstrated in several xenograft mouse models of human cancers, including colorectal cancer [30,31], glioblastoma [31], and breast cancer [32]. These sTRAIL preparations have retained the selective apoptotic activity toward transformed cells, but lack an intrinsic targeting capacity that allows for preferential binding to TRAIL receptors expressed on tumor cells. Moreover, sTRAIL is not very effective in signaling apoptosis in tumor cells that predominantly express TRAIL-R2.

It has been shown that cross-linking of agonistic TRAIL receptors is required to efficiently obtain cell death. In a previous report, Wajant et al. [33] demonstrated that the signaling capacity of sTRAIL for TRAIL-R2 could be restored by genetic fusion to a recombinant antibody fragment (single-chain fragment of variable regions, or scFv) recognizing the tumor stroma marker fibroblast activation protein (FAP). Independently, we developed a TRAIL fusion protein, designated scFvC54:sTRAIL, in which the human scFv antibody fragment C54 is genetically linked to the N-terminus of human sTRAIL [34]. The high-affinity scFvC54 antibody domain specifically targets EGP2 [also known as epithelial cell adhesion molecule (Ep-CAM), or CO17-1a antigen], an established cell surface target antigen overexpressed in a variety of carcinomas. Selective binding to EGP2 results in accretion of scFvC54:sTRAIL at the cell surface of targeted cells only, converting soluble scFvC54:sTRAIL into a membrane-bound form of TRAIL. Subsequently, a surplus of sTRAIL domains displayed on the target cell surface is available for the cross-linking of TRAIL-R2 on neighboring tumor cells, resulting in efficient and target antigen-restricted reciprocal fratricide apoptosis induction. In the present study, we analyzed whether targeting of scFvC54:sTRAIL to EGP2-positive cells can be used to convey a pro–apoptotic bystander effect toward neighboring tumor cells devoid of EGP2 expression, as schematically depicted in Figure 1.

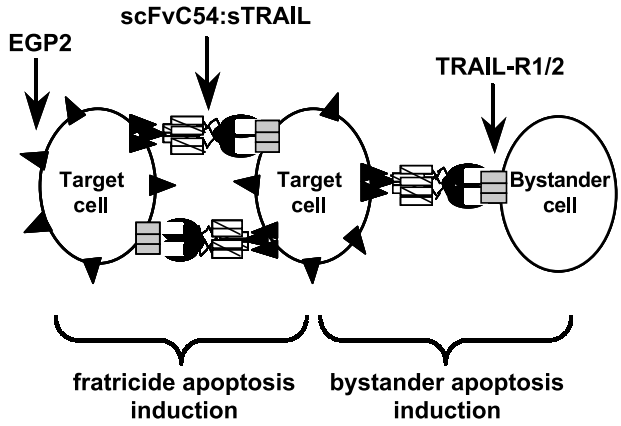

Figure 1. *Target cell and bystander cell apoptosis induction by scFvC54:sTRAIL. Binding of scFvC54:sTRAIL to the abundantly expressed target antigen EGP2 (▲) results in immobilization of scFvC54:sTRAIL at the cell surface of EGP2-positive cells only. Subsequently, membrane-bound scFvC54:sTRAIL induces fratricide apoptosis by reciprocal cross-linking of TRAIL-R1/R2 (▭) on neighboring EGP2-positive target cells. Analogously, immobilized scFvC54:sTRAIL on target cells can induce cross-linking of agonistic TRAIL receptors on the cell surface of a neighboring tumor cell devoid of EGP2 expression, resulting in apoptosis induction of one or more bystander cells (diagram is not to scale).*

Interestingly, we observed an exceptionally potent bystander apoptotic effect of scFvC54:sTRAIL, which critically depended on the presence of EGP2-positive target cells. Bystander apoptosis induction by scFvC54:sTRAIL might be applicable for the treatment of human cancer cells that escape current antibody-based therapy due to partial loss of target antigen expression.

Materials and Methods

Monoclonal Antibodies (MAbs) and scFv Antibody Fragment

MAb MOC31 is a murine IgG1 with high-affinity specificity for human EGP2 [35]. MAb MOC31 was directly labeled with phycoerythrin (PE), yielding MOC31-PE using standard procedures. The anti–EGP2 scFvC54 (kindly provided by Prof. T. Logtenberg, Utrecht University, Utrecht, The Netherlands) has been previously selected from a large semisynthetic phage display library with random human VH–VL pairings and has a VH(G4S)3–VL format [36]. MAb MOC31 and scFvC54 compete for binding to the same epitope on the extracellular domain of EGP2. A multimeric form of the extracellular domain of EGP2 (sEGP2) was produced and purified as described previously [37]. Where indicated, multimeric sEGP2 was used to secondarily cross-link scFvC54:sTRAIL. TRAIL-neutralizing MAb 2E5 was purchased from Alexis (Kordia Life Sciences, Leiden, The Netherlands). MAb 2E5 neutralizes TRAIL activity by binding to an epitope on the extracellular domain of TRAIL that inhibits binding to the various TRAIL receptors.

Cell Lines and EGP2 Transfectants

Human cell lines Jurkat (acute lymphoblastic T-cell leukemia), Ramos (B-cell lymphoma), and U87MG (glioblastoma), all of which are EGP2-negative, were purchased from the

ATCC (Manassas, VA). EGP2-positive variants of the above cell lines were generated by retroviral transduction. In short, EGP2 cDNA was cloned into a retroviral vector derivative of LZRS-pBMN-lacZ [38] (kindly provided by Dr. G. Nolan, Stanford University School of Medicine, San Francisco, CA), yielding LZRS-EGP2-IRES-EGFP. To produce retroviral particles, LZRS-EGP2-IRES-EGFP was transfected into the amphotrophic packaging cell line Phoenix, using Fugene-6 transfection reagent according to the manufacturer's recommendations (Roche Diagnostics, Almere, The Netherlands). Transfected cells were selected by culturing in the presence of 1 μg/ml puromycin, 300 μg/ml hygromycin, and 1 μg/ml diphtheria toxin (BD Biosciences Clontech, Palo Alto, CA). Viral particle-containing supernatant was harvested after 3 days and used to transduce Jurkat, Ramos, and U87MG cells. After overnight incubation, viral particle–containing supernatant was replaced by fresh medium. Transduced cells were subsequently sorted for simultaneous enhanced green fluorescent protein (EGFP) fluorescence and EGP2 expression as detected by MOC31-PE using the MoFlo high-speed cell sorter (Cytomation, Fort Collins, CO). Analogous methods were employed to generate c-FLIPL–encoding retroviral particles, which were used to transduce Ramos cells. Ectopic overexpression of c-$FLIP_L$ in Ramos.c-$FLIP_L$–transduced cells was confirmed by immunoblotting of intracellular protein extracts. All cell lines were cultured at 37°C in humidified 5% CO_2 atmosphere. Suspension cell lines (Jurkat, Jurkat.EGP2, Ramos, Ramos. EGP2, and Ramos.c-$FLIP_L$) were cultured in RPMI (Cambrex, East Rutherford, NJ) supplemented with 15% fetal calf serum (FCS). Adherent cell lines (U87MG and U87MG.EGP2) were cultured in DMEM (Cambrex) supplemented with 10% FCS.

Expression of TRAIL Receptors

Membrane expression levels of TRAIL receptors 1, 2, 3, and 4 were analyzed by flow cytometry using a TRAIL receptor antibody kit purchased from Alexis. Briefly, cells were harvested, washed using serum-free RPMI, and resuspended in 100 μl of fresh medium containing the appropriate primary MAb. Specific binding of the primary antibody was detected using a PE-conjugated secondary antibody (DAKO, Glostrup, Denmark). All antibody incubations were performed at 0°C for 45 minutes and were followed by two washes with serum-free medium.

Production of scFvC54:sTRAIL

The fusion protein scFvC54:sTRAIL, comprising the scFvC54 targeting domain, an intrachain linker, and the sTRAIL effector domain, was produced in Chinese hamster ovary (CHO-K1) cells as previously described [34]. Briefly, the expression plasmid pEE14scFvC54:sTRAIL was transfected to CHO-K1 cells, after which cells were selected for amplified medium secretion of the fusion protein using the glutamine synthetase method as described before [39]. Single cell sorting of transfectants using the MoFlo high-speed cell sorter (Cytomation) identified CHO-K1 clone 70C1 that stably secreted 3.44 μg/ml scFvC54:sTRAIL into the culture medium. Using the same procedures, mock-scFvH22:sTRAIL, directed at the antigen CD64 not present on the cell lines used in this study, was generated and added in experiments where indicated.

Apoptosis Induction Assessed by Viability Assay

Where indicated, apoptosis induction apparent from loss of tumor cell viability was assessed by MTS ([3-(4,5-dimethylthiazol-2-yl)-5-(3-carboxymethoxyphenyl)-2-(4-sulfophenyl]-2H-tetrazolium, inner salt) assay (Promega Benelux BV, Leiden, The Netherlands). Briefly, cells were seeded in flat-bottom 96-well microculture plates at a density of 3×10^4 cells/well in 100 μl of medium. After overnight culture, spent medium was removed and replaced by 200 μl of medium containing various experimental conditions. After 16 hours, MTS assay was performed according to the manufacturer's recommendations. Experimental apoptosis induction was quantified as the percentage apoptosis compared to medium control, which was set at 0% apoptosis. Each experimental and control group consisted of six independent wells.

Apoptosis Induction Assessed by Loss of Mitochondrial Membrane Potential ($\Delta\psi$)

Where indicated, apoptosis induction apparent from loss of $\Delta\psi$ was analyzed using the cell-permeant green fluorescent lipophilic dye DiOC6 (Molecular Probes, Eugene, OR) as previously described [40]. In short, after 16 hours of treatment, cells were harvested by centrifugation (1200*g*, 5 minutes) and incubated for 30 minutes at 37°C with fresh medium containing 0.1 μM DiOC6, washed twice with phosphate-buffered saline (PBS), and analyzed using flow cytometry.

Immunoblot Analysis of Caspase Activation and PARP Cleavage

Where indicated, apoptosis induction apparent from caspase-8 and caspase-3 activation and PARP degradation was assessed by immunoblot analysis using antibodies against active caspase-8 (Cell Signaling Technology, Beverly, MA), active caspase-3 (BD Biosciences, San Jose, CA), and PARP (Santa Cruz Biotechnology, Santa Cruz, CA) respectively. Briefly, cells were seeded in six-well plates at a final concentration of 0.5×10^6 cells/ml and treated as indicated. Cells were harvested by centrifugation (2000*g*, 10 minutes), lysed in lysis buffer (20 mM Tris–HCl, 5.0 mM EDTA, 2.0 mM EGTA, 100 mM NaCl, 0.05% SDS, 0.50% NP-40, 1 mM PMSF, 10 μg/ml aprotein, 10 μg/ml leupeptin, pH 6.8), and sonicated on ice for 2×5 seconds. Cleared supernatants were collected after centrifugation (15,000*g*, 10 minutes) and protein concentration was determined using the Bradford method according to the manufacturer's instructions (BioRad, Hercules, CA). Samples were diluted 1:1 in standard SDS/PAGE loading buffer containing 2-mercapto-ethanol and boiled for 10 minutes. Samples of 30 μg of total protein were loaded and separated using 10% acrylamide SDS-PAGE, followed by electroblot transfer to nitrocellulose. Blots were incubated with the respective primary MAbs and appropriate HRPO-conjugated secondary antibodies. Specific binding of MAbs was detected using ECL (Roche Diagnostics, Indianapolis, IN). All antibody incubations were

performed at room temperature for 1.5 hours in PBS containing 5% bovine serum albumin, followed by three washes with PBS containing 0.1% Tween 20.

Distinctive Fluorescent Labeling of Target and Bystander Cells

Differential cell membrane labeling of target and bystander cells was achieved using the Vybrant Multicolor Cell-Labeling kit (Molecular Probes). EGP2-negative bystander cells were labeled with the red fluorescent dye DiI, whereas the corresponding EGP2-positive target cells were not labeled. Briefly, labeling was performed by incubation of bystander cells (1×10^6 cells/ml in serum-free medium) with 5 μM DiI (37°C, 5 minutes) followed by three subsequent washes with medium (1200*g*, 5 minutes). Pellet was resuspended in medium whereupon the DiI-labeled bystander cells were mixed with nonlabeled target cells at the target-to-bystander ratios indicated at a final concentration of 0.5×10^6 cells/ml. Differential membrane fluorescent characteristics allow the target and bystander cells to be separately evaluated in mixed culture after treatment.

Distinctive Quantification of Apoptosis in Target and Bystander Cells by Loss of $\Delta\psi$

Nonlabeled target cells and DiI-labeled bystander cells were mixed, at the indicated ratios, at a final concentration of 0.5×10^6 cells/well in a 12-well plate. After overnight culture, cell mixtures were treated with scFvC54:sTRAIL (300 ng/ml) for 16 hours in the presence or absence of MAb MOC31 (5 μg/ml), caspase-8 inhibitor Z-IETD-FMK (1 μg/ml) (Calbiochem, San Diego, CA), or TRAIL-neutralizing MAb 2E5 (1 μg/ml). The differential fluorescent characteristics of target and bystander cells were subsequently used to separately evaluate the amount of apoptosis induced in target and bystander cells by measuring the loss of $\Delta\psi$ with the fluorescent dye DiOC6, as described above.

Fluorescence-Activated Cell Sorting (FACS) Sorting of Target and Bystander Cells After Treatment

FACS sorting was applied to separate mixed target cells and bystander cells after treatment with scFvC54:sTRAIL. To this end, DiI-labeled bystander cells (Jurkat) were mixed with an equal amount of unlabeled target cells (Jurkat.EGP2) at a final concentration of 0.5×10^6 cells/ml. This mixed cell culture was treated with scFvC54:sTRAIL (300 ng/ml) for 6 hours in the presence or absence of MAbs MOC31 (5 μg/ml) or 2E5 (1 μg/ml). After treatment, cell mixtures were collected and washed twice in fresh medium precooled at 0°C. Subsequently, 2.5×10^6 cells of both the target and bystander cells were sorted using the MoFlo high-speed cell sorter. The sorted cells were found to be >99% pure and were separately analyzed for apoptotic features by immunoblot as described above.

Fluorescence Microscopy of Bystander Apoptosis Induction

Fluorescent microscopy was used to visualize bystander apoptosis induction in the adherent growing glioblastoma cell line U87MG. U87MG.EGP2 target cells, brightly expressing EGFP, were mixed at a 1:4 ratio with U87MG bystander cells at a final concentration of 0.5×10^6 cells/well on Lab-Tek chamber slides (Nalge Nunc International, Naperville, IL). After overnight culture, spent medium was carefully aspirated and the mixed cell culture was subjected to treatment with scFvC54:sTRAIL (300 ng/ml) for 16 hours, in the presence or absence of MAb MOC31 (5 μg/ml) or MAb 2E5 (1 μg/ml), respectively. After treatment, apoptosis induction apparent from nuclear morphology was analyzed using the DNA-binding dye Hoechst 33342 (Molecular Probes). Both nuclear morphology and EGFP fluorescence were visualized using a Quantimed 600S fluorescence microscope (Leica Camera AG, Solms, Germany).

Quantification of Innocent Bystander Apoptosis in Leukocytes

Leukocytes were isolated from EDTA anticoagulated blood of healthy donors using the ammonium chloride method according to standard procedure. Briefly, blood was diluted eight-fold with cold ammonium chloride buffer and incubated for 10 minutes at 0°C, allowing the lysis of red blood cells. Subsequently, leukocytes were collected by centrifugation (1200*g*, 5 minutes). The above described procedure was repeated to ensure complete lysis of all red blood cells. Isolated leukocytes were resuspended (RPMI, 10% human pool serum) and mixed at a target-to-bystander ratio of 1:1 with target Jurkat.EGP2 cells that were labeled with the green fluorescent dye DiO (Molecular Probes). Mixed cultures were treated for 16 hours with scFvC54:sTRAIL in the presence or absence of MAb MOC31 or MAb2E5. The degree of apoptosis induction after treatment was analyzed by addition of the fluorescent DNA-binding dye propidium iodide (PI) and quantification of the percentage of PI-positive cells using flow cytometry.

Results

TRAIL-R Expression in EGP2-Transduced Cell Lines

Flow cytometric analysis of the retrovirally transduced cell lines Jurkat.EGP2, Ramos.EGP2, and U87MG.EGP2 revealed a strong homogeneous cell surface expression of EGP2 and intracellular EGFP fluorescence (data not shown). No significant differences in TRAIL receptor expression patterns were found between parental and EGP2-transduced cell lines (Table 1).

Target Cell–Restricted Apoptosis Induction by scFvC54:sTRAIL

EGP2-negative bystander cells (Jurkat, Ramos, and U87MG) were not susceptible to apoptosis induction by scFvC54:sTRAIL. After prolonged treatment (16 hours) with 300 ng/ml scFvC54:sTRAIL, cell cultures contained only low percentages of apoptotic cells (Figure 2*A*; 5%, 10%, and 3%, for Jurkat, Ramos, and U87MG, respectively). When treatment was performed in the presence of multimeric soluble EGP2 (3.5 μg/ml), which secondarily cross-links scFvC54:sTRAIL, a strong increase in the percentages of apoptotic

Table 1. Flow Cytometric Analysis of TRAIL Receptor Expression on Target and Bystander Cells.

Cell Line	TRAIL-R1	TRAIL-R2	TRAIL-R3	TRAIL-R4
Ramos	*	*	nd	†
Ramos.EGP2	*	*	nd	†
Jurkat	nd	*	nd	†
Jurkat.EGP2	nd	*	nd	†
U87MG	†	‡	†	†
U87MG.EGP2	†	†	†	†

EGP2-positive target cells and EGP2-negative bystander cells were analyzed for TRAIL receptor expression.
Expression of TRAIL receptors was classified as not detectable (nd) when MFI was below 5.
*50 < MFI < 125.
† 5 < MFI < 25.
‡ 25 < MFI < 50.

cells was observed (92%, 84%, and 70% for Jurkat, Ramos, and U87MG, respectively).

Treatment of EGP2-positive target cells (Jurkat.EGP2, Ramos.EGP2, and U87MG.EGP2) with 300 ng/ml scFvC54:sTRAIL induced a strong increase in percentage of apoptotic cells (Figure 2*B*; 71%, 67%, and 65%, respectively). Treatment of these EGP2-positive cells in the presence of EGP2-blocking MAb MOC31 strongly inhibited apoptosis induction (16%, 13%, and 5%, for Jurkat.EGP2, Ramos.EGP2, and U87MG.EGP2, respectively). Interestingly, although levels of TRAIL receptor expression were comparable for both parental and EGP2-transduced cell lines, the sensitivity to apoptosis induction by scFvC54:sTRAIL was somewhat reduced in the EGP2- transduced cell lines. Reduced sensitivity of EGP2-transduced cells may be related to the retroviral transduction procedure of these cell lines, or the ectopic overexpression of EGP2.

Distinctive Quantification of Apoptosis Induction in Target and Bystander Cells

When mixed cultures of Jurkat.EGP2 target cells and Jurkat bystander cells were treated with scFvC54:sTRAIL, strong apoptosis induction was observed in Jurkat.EGP2 target cells, ranging from 55% at target-to-bystander ratio of 7:3 to 20% at ratio 1:100 (Figure 3*A*). Apoptosis induction in Jurkat bystander cells ranged from 80% at ratio 7:3 to 17% at the remarkably low ratio 1:100 (Figure 3*B*). Treatment of bystander cells alone resulted in marginal induction of apoptosis (7%). Percentages of apoptotic cells were strongly reduced in both target and bystander cell populations when treatment was performed in the presence of EGP2-blocking MAb MOC31 (Figure 3, *A* and *B*). Analogously, treatment with scFvC54:sTRAIL in the presence of TRAIL-neutralizing MAb 2E5 resulted in complete abrogation of apoptosis (Figure 3, *A* and *B*). Furthermore, when mixed cultures of target and bystander cells were treated with the mock-scFvH22:sTRAIL fusion protein containing the antibody fragment domain scFvH22 of irrelevant specificity, no apoptosis induction was found in Jurkat.EGP2 target or Jurkat bystander cells (Figure 3*C*). Similar experiments with mixed cultures of Ramos.EGP2 and Ramos, and the adherent cell lines U87MG.EGP2 and U87MG, further confirmed that treatment with scFvC54:sTRAIL potently induced both target and bystander apoptosis, whereas treatment with mock-scFvH22:sTRAIL did not lead to significant apoptosis induction in target or bystander cells (Figure 3*C*).

Target and Bystander Apoptosis Induction Is Caspase-8–Dependent

In a mixed culture of Ramos.EGP2 target cells and Ramos bystander cells (ratio 2:3), treatment with scFvC54:sTRAIL resulted in bystander apoptosis induction up to 65% (Figure 4*A*). However, treatment in the presence of the specific caspase-8 inhibitor Z-IETD-FMK strongly inhibited apoptosis induction in both target and bystander cells (Figure 4*A*; 15% and 17%, respectively). Moreover, treatment of a mixed culture of target cells (Ramos.EGP2) and bystander cells ectopically overexpressing the caspase-8

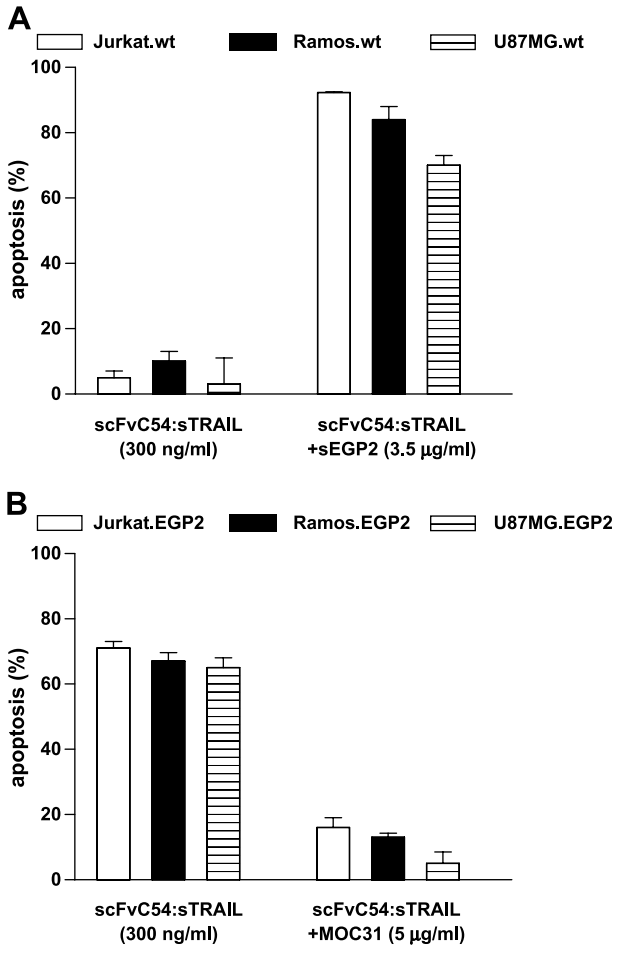

Figure 2. *Target cell–restricted apoptosis induction by scFvC54:sTRAIL. (A) EGP2-negative bystander cells (Jurkat, Ramos, and U87MG) were treated with scFvC54:sTRAIL alone to determine sensitivity to apoptosis induction by noncross-linked scFvC54:sTRAIL. Additionally, cells were treated with scFvC54:sTRAIL in the presence of multimeric sEGP2, which secondarily cross-links scFvC54:sTRAIL, to determine intrinsic sensitivity to cross-linked scFvC54:sTRAIL. (B) EGP2-positive target cells (Jurkat.EGP2, Ramos. EGP2, and U87MG.EGP2) were treated with scFvC54:sTRAIL for 16 hours in the presence or absence of target antigen–competing MAb MOC31. Apoptosis induction was assessed by MTS assay as described in Materials and Methods section. All values indicated in the graphs are the mean ± SEM of four independent experiments.*

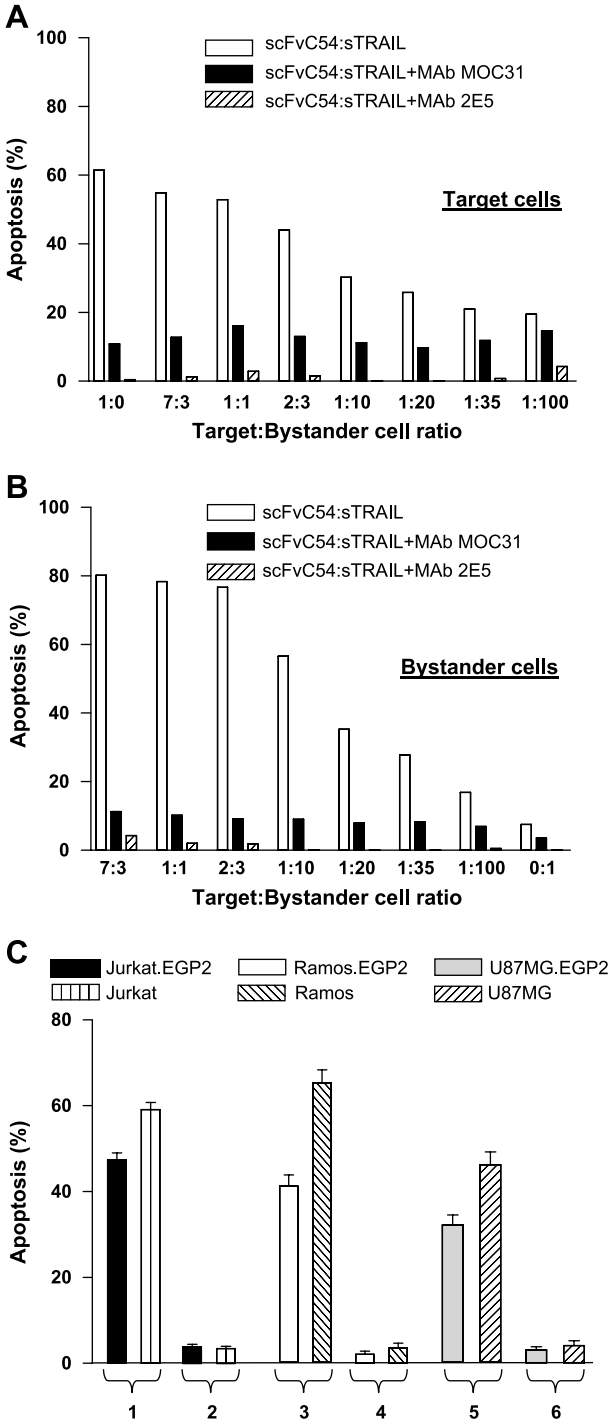

Figure 3. *Separate evaluation of target cell and bystander cell apoptosis induction by scFvC54:sTRAIL. Jurkat.EGP2 target and Jurkat bystander cells were mixed at different target-to-bystander ratios and treated for 16 hours with 300 ng/ml scFvC54:sTRAIL in the presence or absence of MAb MOC31 (5 μg/ml) or MAb 2E5 (1 μg/ml). After treatment, cells were harvested and apoptosis induction was separately evaluated in (A) Jurkat.EGP2 target cells and (B) Jurkat bystander cells. (C) Target antigen–dependent fratricide and bystander apoptosis induction. Mixed cultures of target and bystander cell combinations Jurkat.EGP2/Jurkat, Ramos.EGP2/Ramos, and U87MG.EGP2/U87MG. EGP2 (at target-to-bystander ratio of 2:3) were treated with 300 ng/ml scFvC54:sTRAIL (bars 1, 3, and 5), or with equal amounts of a scFv:sTRAIL fusion protein of irrelevant specificity (mock-scFvH22:sTRAIL) (bars 2, 4, and 6). Apoptosis induction was separately evaluated in target and bystander cells by loss of $\Delta\psi$ as described in Materials and Methods section. All values indicated in the graphs are mean ± SEM of four independent experiments.*

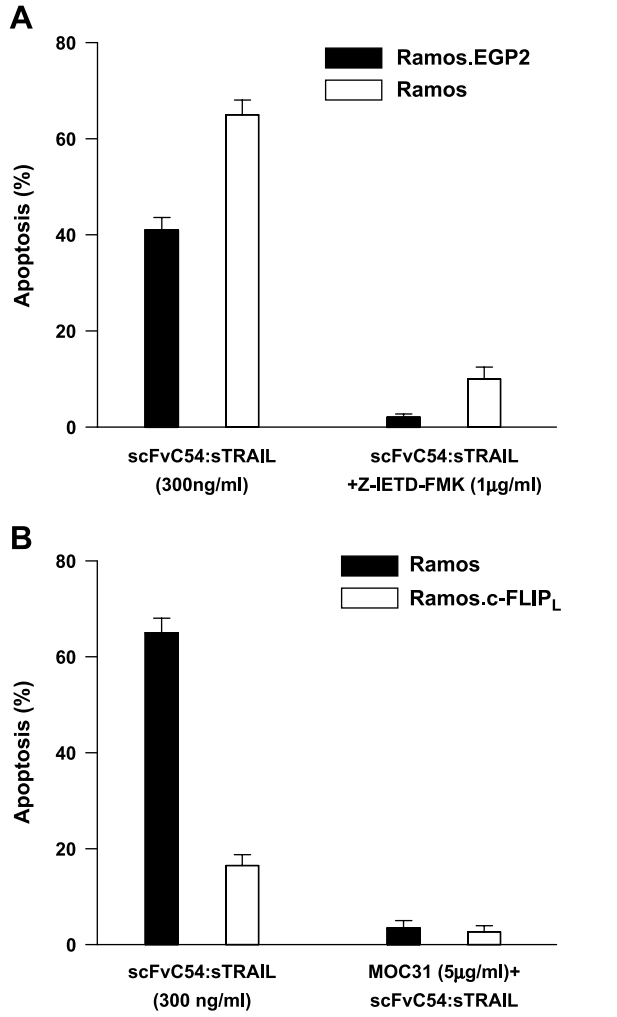

Figure 4. *(A) Target cell and bystander cell apoptosis induction by scFvC54:sTRAIL is caspase-8–specific. Ramos.EGP2 target cells and Ramos bystander cells were mixed at target-to-bystander ratio of 2:3 and treated with scFvC54:sTRAIL in the presence or absence of caspase-8 inhibitor, Z-IETD-FMK. After 16 hours, cells were harvested and apoptosis induction was separately evaluated by loss of $\Delta\psi$ in Ramos.EGP2 target cells and Ramos bystander cells. (B) Ramos bystander cells ectopically overexpressing c-FLIP$_L$ are largely insensitive to bystander apoptosis induction. Ramos.EGP2 target cells were mixed at 2:3 target-to-bystander ratio with either parental Ramos bystander cells or Ramos bystander cells ectopically overexpressing cFLIP$_L$ (Ramos cFLIP$_L$). Mixed cultures were subsequently treated with 300 ng/ml scFvC54:sTRAIL in the presence or absence of MAb MOC31, after which apoptosis induction was evaluated in bystander Ramos or Ramos.cFLIP$_L$ by loss of $\Delta\psi$. All values indicated in the graph are mean ± SEM of four independent experiments.*

inhibitor c-FLIP$_L$ (Ramos.c-FLIP$_L$) indicated that Ramos.c-FLIPL bystander cells are largely resistant to the pro–apoptotic bystander effect of scFvC54:sTRAIL (Figure 4*B*; 17%). The residual apoptosis induction observed for Ramos.c-FLIP$_L$ bystander cells could be specifically inhibited by coincubation with MAb MOC31.

Immunoblot Analysis of FACS-Sorted Target and Bystander Cells

Posttreatment sorting of a mixed culture of Jurkat.EGP2 target and Jurkat bystander cells (ratio 1:1) allowed for the separate evaluation of apoptotic features in target and

bystander cells. Treatment with scFvC54:sTRAIL induced a clear activation of caspase-8 and caspase-3 in both Jurkat.EGP2 target cells (Figure 5*A*, *lane 2*) and Jurkat bystander cells (Figure 5*B*, *lane 2*). Activation of caspase-3 was accompanied by cleavage of its target protein PARP (Figure 5, *A* and *B*, *lane 2*). Treatment in the presence of MAb MOC31 or MAb 2E5 inhibited caspase activation and PARP cleavage in both target and bystander cells (Figure 5, *A* and *B*, *lanes 3 and 4*, respectively). Neither caspase activation nor PARP cleavage was observed when Jurkat bystander cells were treated in the absence of Jurkat.EGP2 target cells, even when treatment was prolonged to 24 hours (data not shown).

Fluorescent Microscopy of Bystander Apoptosis Induction

Microscopic evaluation of untreated mixed cultures revealed that adherent U87MG.EGP2 target cells and U87MG bystander cells were interconnected by cellular protrusions (Figure 6*A*). Protrusions coming from U87MG.EGP2 target cells can be appreciated due to the EGFP fluorescence present in the cytoplasm of these cells. When a mixed culture of U87MG.EGP2 target cells and U87MG bystander cells (ratio 1:4) was treated with 300 ng/ml scFvC54:sTRAIL for 16 hours, pronounced apoptotic morphologic features such as membrane blebbing and nuclear condensation were visible in both target and bystander cells. The efficacy of the bystander effect was apparent from the fact that apoptotic morphology was observed in almost all U87MG bystander cells (Figure 6*B*). Identical treatment in the presence of either MAb MOC31 or MAb 2E5 strongly inhibited the appearance of apoptotic morphology in both U87MG.EGP2 target cells and U87MG bystander cells (Figure 6, *C* and *D*).

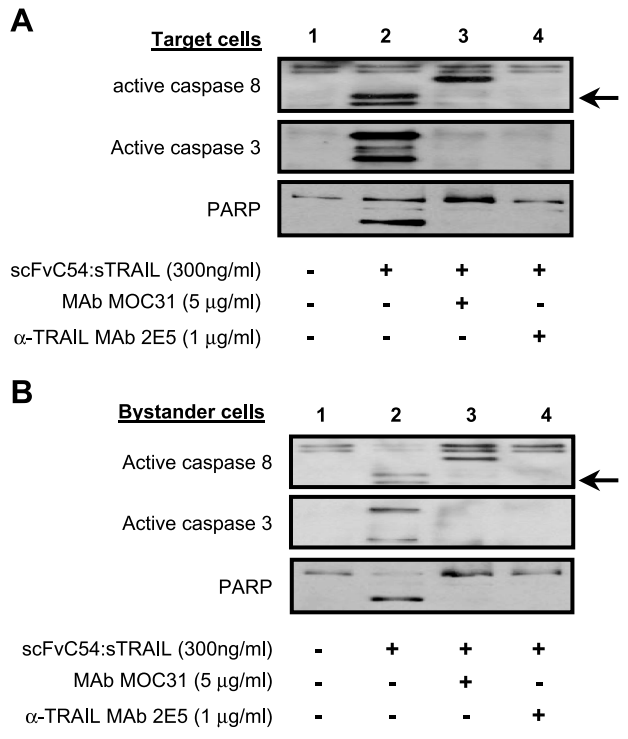

Figure 5. *Separate evaluation of caspase activation and PARP cleavage in Jurkat.EGP2 target cells and Jurkat bystander cells. Jurkat.EGP2 target cells and Jurkat bystander cells were mixed at target-to-bystander ratio of 1:1 and treated for 6 hours with scFvC54:sTRAIL in the presence or absence of MAb MOC31 or MAb 2E5. After treatment, Jurkat.EGP2 target and Jurkat bystander cells were separated by high-speed cell sorting, after which (A) Jurkat.EGP2 target cells and (B) Jurkat bystander cells were separately analyzed by immunoblot for caspase-8 activation, caspase-3 activation, and PARP degradation. Arrows indicate bands corresponding to cleaved caspase-8. Of note, in the caspase-8 blot of both Jurkat.EGP2 target cells and Jurkat bystander cells, a specific band derived from the heavy chain of MAb MOC31 is also visible.*

No Innocent Bystander Apoptosis in Isolated Leukocytes

Treatment of mixed cultures of isolated leukocytes (innocent bystander cells) and Jurkat.EGP2 cells with scFvC54:sTRAIL did not lead to any significant induction of apoptosis in the bystander leukocytes (Figure 7), whereas strong apoptosis up to 46% was observed in Jurkat.EGP2 target cells. Apoptosis in Jurkat.EGP2 was specifically inhibited when treatment was performed in the presence of MAb MOC31 or MAb 2E5.

Discussion

It has been shown that cross-linking of TRAIL receptors is crucial for the efficient induction of apoptosis in tumor cells. Previously, we reported on target cell–restricted fratricide apoptosis induction by the fusion protein scFvC54:sTRAIL due to the efficient cross-linking of agonistic TRAIL receptors TRAIL-R1 and TRAIL-R2 [34]. In the present study, we analyzed whether selective binding of scFvC54:sTRAIL to EGP2-positive tumor cells could further be used to cross-link TRAIL receptors on neighboring tumor cells devoid of EGP2 expression using mixed cell culture experiments. To this end, we selected a series of cell lines that represent three major human malignancies: acute lymphoblastic T-cell leukemia (Jurkat), B-cell lymphoma (Ramos), and glioblastoma multiforme (U87MG), all of which are EGP2-negative and generated EGP2-positive target cells thereof by retroviral transduction. Furthermore, we devised a method that allowed for distinctive evaluation of apoptosis in target and bystander cells.

All EGP2-negative bystander cell types used were fully resistant to prolonged treatment with scFvC54:sTRAIL (16 hours, 300 ng/ml). However, when mixed cultures of EGP2-positive target cells and corresponding EGP2-negative bystander cells were treated, potent pro–apoptotic effects of up to 80% apoptosis induction were achieved in EGP2-negative bystander cells (Figure 3*A*). Pro–apoptotic bystander activity of scFvC54:sTRAIL was observed for both suspension tumor cell types (Jurkat and Ramos) and adherent U87MG glioblastoma cells (Figure 3*C*).

Treatment of mixed cultures containing as little as 1% of EGP2-positive target cells still showed significant apoptosis induction of up to 17% in EGP2-negative bystander cells. This clearly indicated that significant pro–apoptotic bystander activity of scFvC54:sTRAIL can be achieved at low target-to-bystander cell ratios. Treatment in the presence of an EGP2-blocking antibody or a TRAIL-neutralizing antibody strongly inhibited apoptosis induction in both target and bystander cells at all ratios analyzed (Figure 3, *A* and *B*).

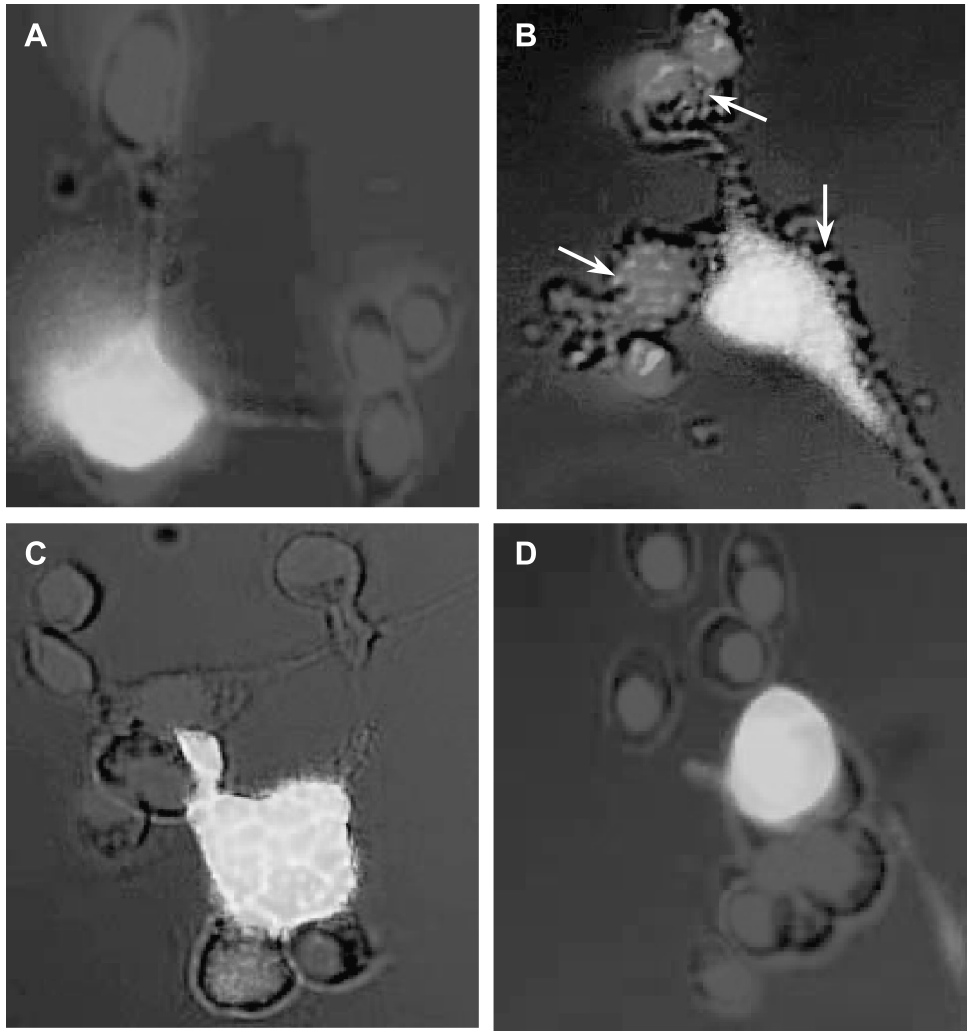

Figure 6. *Visualization of bystander apoptosis by fluorescence microscopy. U87MG.EGP2 target cells and U87MG bystander cells were mixed at a target-to-bystander ratio of 1:4 and precultured on chamber slides. Subsequently, the mixed cultures were subjected for 16 hours to treatment with (A) medium, (B) scFvC54:sTRAIL (300 ng/ml), (C) MAb MOC31 (5 μg/ml) + scFvC54:sTRAIL, and (D) MAb 2E5 (1 μg/ml) + scFvC54:sTRAIL. After treatment, cells were stained using the nuclear stain Hoechst and analyzed for characteristic apoptotic morphology. Target and bystander cells could be distinctly discriminated due to the expression of green fluorescent protein by U87MG.EGP2 target cells only.*

When treatment was performed using identical amounts of a scFv:sTRAIL fusion protein of irrelevant specificity (mock-scFvH22:sTRAIL), no induction of apoptosis was observed (Figure 3*C*). Furthermore, apoptosis induction was specifically absent in bystander cells that ectopically overexpressed c-FLIP$_L$, a specific inhibitor of death receptor–induced apoptosis (Figure 4*B*). Immunoblot analysis of posttreatment-sorted target and bystander cells demonstrated identical activation profiles of caspase-3 and caspase-8, and cleavage of PARP (Figure 5, *A* and *B*). Together, these results all indicated that both fratricide and bystander apoptosis induction by scFvC54:sTRAIL are mediated by target cell–dependent intracellular cross-linking of agonistic TRAIL receptors.

Microscopic evaluation of a mixed culture (ratio 1:4) of adherent U87MG.EGP2 target cells and U87MG bystander cells treated with scFvC54:sTRAIL visualized pronounced apoptotic morphologic features (nuclear condensation and membrane blebbing) in both target and bystander cells. The strong bystander effect observed here might partly be due to the fact that U87MG cells have extensive cellular protrusions that appear to make multiple intracellular connections even to more distant cells (Figure 6*A*). Possibly, this particular cell morphology influences TRAIL receptor cross-linking by scFvC54:sTRAIL between interconnected target cells and bystander cells. It is tentative to speculate that scFv:sTRAIL treatment of target cells with more extensive cellular protrusions may induce apoptosis in more distant bystander cells.

As discussed above, we analyzed the pro–apoptotic bystander effect by scFvC54:sTRAIL down to extremely low target-to-bystander cell ratios. We noticed that when treatment was performed at ratios < 1:10, apoptosis induction in the target cells was partly inhibited (Figure 3*A*). It appears that the presence of a vast majority of bystander cells reduces direct cellular contacts between EGP2-positive target cells, subsequently reducing fratricide apoptosis induction of these cells. The inhibitory effect of bystander cells on fratricide apoptosis induction in target cells was not

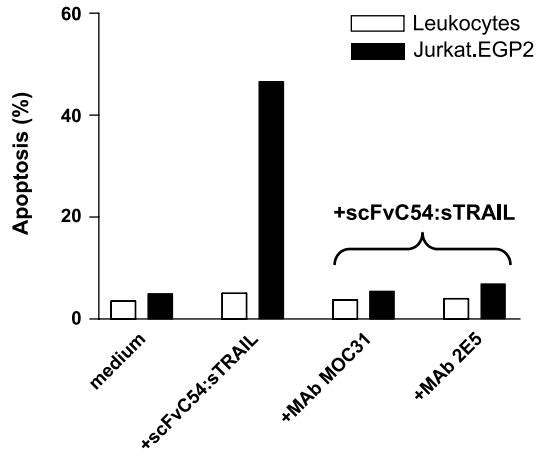

Figure 7. *No innocent bystander cell apoptosis in isolated leukocytes. Isolated leukocytes were mixed with Jurkat.EGP2 target cells at a target-to-bystander ratio of 1:1. Mixed cultures were then treated for 16 hours with scFvC54:sTRAIL in the presence or absence of MAb MOC31 or MAb 2E5. Apoptosis induction was separately analyzed for leukocytes and Jurkat.EGP2 using PI staining, as described in Materials and Methods section.*

observed at higher—and possibly more realistic—target-to-bystander cell ratios.

Previously, bystander effects have been observed in antibody-directed enzyme prodrug therapy (ADEPT) [41] and virus-directed enzyme prodrug therapy (VDEPT) [13,42], therapeutic approaches that target a nonhuman prodrug-converting enzyme into tumor cells and involve the transfer and diffusion of toxic metabolites from one cell to another. Usually, the toxic metabolites produced using these strategies cannot freely transit the cell membrane. Consequently, these bystander effects chiefly depend on gap junctional intracellular communication (GJIC) between target and bystander tumor cells [14,43–45]. Unfortunately, most cancer cells lack functional GJIC. The bystander apoptosis activity described here for scFvC54:sTRAIL does not require internalization, enzymatic conversion, diffusion, or communication (GJIC) between target and bystander cells.

An additional problem in both ADEPT and VDEPT appears to be the preferential killing of targeted cells due to their relative high intracellular concentration of the toxic metabolite, resulting in a decreased bystander effect. In contrast, the bystander activity of scFvC54:sTRAIL is likely to be maintained during the whole process of target cell apoptosis induction. Moreover, apoptosis of a given target cell can yield numerous minute apoptotic bodies with intact EGP2-positive cellular membranes. *In vitro*, target cell–derived apoptotic bodies displaying scFvC54:sTRAIL might continue to contribute to the cross-linking of TRAIL receptors and potentially disseminate the bystander effect to more distant tumor cells. The presence and subsequent contribution of such apoptotic bodies to the bystander effect studied here remain to be clarified. However, *in vivo*, it is likely that phagocytosing cells of the immune system rapidly scavenge such apoptotic bodies before additional bystander apoptosis induction is initiated.

We wondered whether the potent pro–apoptotic bystander effect of scFvC54:sTRAIL might also result in the killing of "innocent bystander" cells such as normal blood cells. Therefore, we added freshly isolated leukocytes to various bystander experiments and found no significant signs of apoptosis induction in the various blood cell types (Figure 7). This indicates that, at least in this experimental setting, scFvC54:sTRAIL has retained its tumor-selective apoptosis activity with no signs of innocent bystander apoptosis induction. Nevertheless, from the present study, it cannot be excluded that scFvC54:sTRAIL might exert toxic or innocent bystander effects toward other normal cells and tissues. Toxicity studies of scFvC54:sTRAIL can possibly be performed in our human EGP2 transgenic mouse model [46] in which human EGP2 expression displays authentic expression patterns in mouse epithelia. In conclusion, this is the first example of target cell–dependent bystander apoptotic activity by a scFv:sTRAIL fusion protein. Further development of this new principle is warranted for TRAIL and antibody-based therapy of human cancers that escape current antibody-based therapy due to heterogeneous target antigen expression.

Acknowledgements

We thank Geert Mesander and Jelleke Dokter-Fokkens for their excellent technical assistance.

References

[1] Rehwald U, Schulz H, Reiser M, Sieber M, Staak JO, Morschhauser F, Driessen C, Rudiger T, Muller-Hermelink K, Diehl V, and Engert A (2003). Treatment of relapsed CD20$^+$ Hodgkin lymphoma with the monoclonal antibody rituximab is effective and well tolerated: results of a phase 2 trial of the German Hodgkin Lymphoma Study Group. *Blood* **101,** 420–424.

[2] Montemurro F, Choa G, Faggiuolo R, Sperti E, Capaldi A, Donadio M, Minischetti M, Salomone A, Vietti-Ramus G, Alabiso O, and Aglietta M (2003). Safety and activity of docetaxel and trastuzumab in HER2 overexpressing metastatic breast cancer: a pilot phase II study. *Am J Clin Oncol* **26,** 95–97.

[3] Emrich JG, Brady LW, Quang TS, Class R, Miyamoto C, Black P, and Rodeck U (2002). Radioiodinated (I-125) monoclonal antibody 425 in the treatment of high grade glioma patients: ten-year synopsis of a novel treatment. *Am J Clin Oncol* **25,** 541–546.

[4] Kennedy GA, Tey SK, Cobcroft R, Marlton P, Cull G, Grimmett K, Thomson D, and Gill D (2002). Incidence and nature of CD20-negative relapses following rituximab therapy in aggressive B-cell non-Hodgkin's lymphoma: a retrospective review. *Br J Haematol* **119,** 412–416.

[5] Davis TA, Czerwinski DK, and Levy R (1999). Therapy of B-cell lymphoma with anti–CD20 antibodies can result in the loss of CD20 antigen expression. *Clin Cancer Res* **5,** 611–615.

[6] Birhiray RE, Shaw G, Guldan S, Rudolf D, Delmastro D, Santabarbara P, and Brettman L (2002). Phenotypic transformation of CD52(pos) to CD52(neg) leukemic T cells as a mechanism for resistance to CAMPATH-1H. *Leukemia* **16,** 861–864.

[7] Coons SW, Johnson PC, and Shapiro JR (1995). Cytogenetic and flow cytometry DNA analysis of regional heterogeneity in a low grade human glioma. *Cancer Res* **55,** 1569–1577.

[8] Houghton AN, Real FX, Davis LJ, Cordon-Cardo C, and Old LJ (1987). Phenotypic heterogeneity of melanoma. Relation to the differentiation program of melanoma cells. *J Exp Med* **165,** 812–829.

[9] Scheck AC, Shapiro JR, Coons SW, Norman SA, and Johnson PC (1996). Biological and molecular analysis of a low-grade recurrence of a glioblastoma multiforme. *Clin Cancer Res* **2,** 187–199.

[10] Weber RG, Sommer C, Albert FK, Kiessling M, and Cremer T (1996). Clinically distinct subgroups of glioblastoma multiforme studied by comparative genomic hybridization. *Lab Invest* **74,** 108–119.

[11] Albino AP, Lloyd KO, Houghton AN, Oettgen HF, and Old LJ (1981). Heterogeneity in surface antigen and glycoprotein expression of cell lines derived from different melanoma metastases of the same

patient. Implications for the study of tumor antigens. *J Exp Med* **154,** 1764–1778.
[12] Owonikoko T, Rees M, Gabbert HE, and Sarbia M (2002). Intratumoral genetic heterogeneity in Barrett adenocarcinoma. *Am J Clin Pathol* **117,** 558–566.
[13] Friedlos F, Davies L, Scanlon I, Ogilvie LM, Martin J, Stribbling SM, Spooner RA, Niculescu-Duvaz I, Marais R, and Springer CJ (2002). Three new prodrugs for suicide gene therapy using carboxypeptidase G2 elicit bystander efficacy in two xenograft models. *Cancer Res* **62,** 1724–1729.
[14] Asklund T, Appelskog IB, Ammerpohl O, Langmoen IA, Dilber MS, Aints A, Ekstrom TJ, and Almqvist PM (2003). Gap junction–mediated bystander effect in primary cultures of human malignant gliomas with recombinant expression of the *HSVtk* gene. *Exp Cell Res* **284,** 185–195.
[15] Hyer ML, Sudarshan S, Schwartz DA, Hannun Y, Dong JY, and Norris JS (2003). Quantification and characterization of the bystander effect in prostate cancer cells following adenovirus-mediated FasL expression. *Cancer Gene Ther* **10,** 330–339.
[16] Kagawa S, He C, Gu J, Koch P, Rha SJ, Roth JA, Curley SA, Stephens LC, and Fang B (2001). Antitumor activity and bystander effects of the tumor necrosis factor–related apoptosis-inducing ligand (TRAIL) gene. *Cancer Res* **61,** 3330–3338.
[17] Seol JY, Park KH, Hwang CI, Park WY, Yoo CG, Kim YW, Han SK, Shim YS, and Lee CT (2003). Adenovirus-TRAIL can overcome TRAIL resistance and induce a bystander effect. *Cancer Gene Ther* **10,** 540–548.
[18] Huang X, Lin T, Gu J, Zhang L, Roth JA, Liu J, and Fang B (2003). Cell to cell contact required for bystander effect of the TNF-related apoptosis-inducing ligand (TRAIL) gene. *Int J Oncol* **22,** 1241–1245.
[19] Wiley SR, Schooley K, Smolak PJ, Din WS, Huang CP, Nicholl JK, Sutherland GR, Smith TD, Rauch C, and Smith CA (1995). Identification and characterization of a new member of the TNF family that induces apoptosis. *Immunity* **3,** 673–682.
[20] Pitti RM, Marsters SA, Ruppert S, Donahue CJ, Moore A, and Ashkenazi A (1996). Induction of apoptosis by Apo-2 ligand, a new member of the tumor necrosis factor cytokine family. *J Biol Chem* **271,** 12687–12690.
[21] Peter ME (2000). The TRAIL DISCussion: it is FADD and caspase-8! *Cell Death Differ* **7,** 759–760.
[22] Kischkel FC, Hellbardt S, Behrmann I, Germer M, Pawlita M, Krammer PH, and Peter ME (1995). Cytotoxicity-dependent APO-1 (Fas/CD95)–associated proteins form a death-inducing signaling complex (DISC) with the receptor. *EMBO J* **14,** 5579–5588.
[23] Kischkel FC, Lawrence DA, Chuntharapai A, Schow P, Kim KJ, and Ashkenazi A (2000). Apo2L/TRAIL–dependent recruitment of endogenous FADD and caspase-8 to death receptors 4 and 5. *Immunity* **12,** 611–620.
[24] Sprick MR, Rieser E, Stahl H, Grosse-Wilde A, Weigand MA, and Walczak H (2002). Caspase-10 is recruited to and activated at the native TRAIL and CD95 death-inducing signalling complexes in a FADD-dependent manner but can not functionally substitute caspase-8. *EMBO J* **21,** 4520–4530.
[25] Sprick MR, Weigand MA, Rieser E, Rauch CT, Juo P, Blenis J, Krammer PH, and Walczak H (2000). FADD/MORT1 and caspase-8 are recruited to TRAIL receptors 1 and 2 and are essential for apoptosis mediated by TRAIL receptor 2. *Immunity* **12,** 599–609.
[26] Chinnaiyan AM, O'Rourke K, Tewari M, and Dixit VM (1995). FADD, a novel death domain-containing protein, interacts with the death domain of Fas and initiates apoptosis. *Cell* **81,** 505–512.
[27] Kischkel FC, Lawrence DA, Tinel A, LeBlanc H, Virmani A, Schow P, Gazdar A, Blenis J, Arnott D, and Ashkenazi A (2001). Death receptor recruitment of endogenous caspase-10 and apoptosis initiation in the absence of caspase-8. *J Biol Chem* **276,** 46639–46646.
[28] Wang J, Chun HJ, Wong W, Spencer DM, and Lenardo MJ (2001). Caspase-10 is an initiator caspase in death receptor signaling. *Proc Natl Acad Sci USA* **98,** 13884–13888.
[29] Muhlenbeck F, Schneider P, Bodmer JL, Schwenzer R, Hauser A, Schubert G, Scheurich P, Moosmayer D, Tschopp J, and Wajant H (2000). The tumor necrosis factor–related apoptosis-inducing ligand receptors TRAIL-R1 and TRAIL-R2 have distinct cross-linking requirements for initiation of apoptosis and are non-redundant in JNK activation. *J Biol Chem* **275,** 32208–32213.
[30] Ashkenazi A, Pai RC, Fong S, Leung S, Lawrence DA, Marsters SA, Blackie C, Chang L, McMurtrey AE, Hebert A, DeForge L, Koumenis IL, Lewis D, Harris L, Bussiere J, Koeppen H, Shahrokh Z, and Schwall R (1999). Safety and antitumor activity of recombinant soluble Apo2 ligand. *J Clin Invest* **104,** 155–162.
[31] Roth W, Isenmann S, Naumann U, Kugler S, Bahr M, Dichgans J, Ashkenazi A, and Weller M (1999). Locoregional Apo2L/TRAIL eradicates intracranial human malignant glioma xenografts in athymic mice in the absence of neurotoxicity. *Biochem Biophys Res Commun* **265,** 479–483.
[32] Walczak H, Miller RE, Ariail K, Gliniak B, Griffith TS, Kubin M, Chin W, Jones J, Woodward A, Le T, Smith C, Smolak P, Goodwin RG, Rauch CT, Schuh JC, and Lynch DH (1999). Tumoricidal activity of tumor necrosis factor–related apoptosis-inducing ligand *in vivo*. *Nat Med* **5,** 157–163.
[33] Wajant H, Moosmayer D, Wuest T, Bartke T, Gerlach E, Schonherr U, Peters N, Scheurich P, and Pfizenmaier K (2001). Differential activation of TRAIL-R1 and -2 by soluble and membrane TRAIL allows selective surface antigen–directed activation of TRAIL-R2 by a soluble TRAIL derivative. *Oncogene* **20,** 4101–4106.
[34] Bremer E, Kuijlen J, Samplonius D, Walczak H, de Leij L, and Helfrich W (2004). Target cell–restricted and –enhanced apoptosis induction by a scFv:sTRAIL fusion protein with specificity for the pancarcinoma-associated antigen EGP2. *Int J Cancer* **109,** 281–290.
[35] Helfrich W, Koning PW, The TH, and de Leij L (1994). Epitope mapping of SCLC-cluster-2 MAbs and generation of antibodies directed against new EGP-2 epitopes. *Int J Cancer Suppl* **8,** 64–69.
[36] Huls GA, Heijnen IA, Cuomo ME, Koningsberger JC, Wiegman L, Boel E, van der Vuurst de Vries AR, Loyson SA, Helfrich W, Berge Henegouwen GP, van Meijer M, de Kruif J, and Logtenberg T (1999). A recombinant, fully human monoclonal antibody with antitumor activity constructed from phage-displayed antibody fragments. *Nat Biotechnol* **17,** 276–281.
[37] Helfrich W, Van Geel M, The TH, and de Leij L (1994). Detection of a putative 30-kDa ligand of the cluster-2 antigen. *Int J Cancer Suppl* **8,** 70–75.
[38] Kinsella TM and Nolan GP (1996). Episomal vectors rapidly and stably produce high-titer recombinant retrovirus. *Hum Gene Ther* **7,** 1405–1413.
[39] Cockett MI, Bebbington CR, and Yarranton GT (1990). High level expression of tissue inhibitor of metalloproteinases in Chinese hamster ovary cells using glutamine synthetase gene amplification. *Biotechnology (New York)* **8,** 662–667.
[40] Quillet-Mary A, Jaffrezou JP, Mansat V, Bordier C, Naval J, and Laurent G (1997). Implication of mitochondrial hydrogen peroxide generation in ceramide-induced apoptosis. *J Biol Chem* **272,** 21388–21395.
[41] Cheng TL, Wei SL, Chen BM, Chern JW, Wu MF, Liu PW, and Roffler SR (1999). Bystander killing of tumour cells by antibody-targeted enzymatic activation of a glucuronide prodrug. *Br J Cancer* **79,** 1378–1385.
[42] Freeman SM, Abboud CN, Whartenby KA, Packman CH, Koeplin DS, Moolten FL, and Abraham GN (1993). The "bystander effect": tumor regression when a fraction of the tumor mass is genetically modified. *Cancer Res* **53,** 5274–5283.
[43] Mesnil M, Piccoli C, Tiraby G, Willecke K, and Yamasaki H (1996). Bystander killing of cancer cells by herpes simplex virus thymidine kinase gene is mediated by connexins. *Proc Natl Acad Sci USA* **93,** 1831–1835.
[44] Elshami AA, Saavedra A, Zhang H, Kucharczuk JC, Spray DC, Fishman GI, Amin KM, Kaiser LR, and Albelda SM (1996). Gap junctions play a role in the "bystander effect" of the herpes simplex virus thymidine kinase/ganciclovir system *in vitro*. *Gene Ther* **3,** 85–92.
[45] Dilber MS, Abedi MR, Christensson B, Bjorkstrand B, Kidder GM, Naus CC, Gahrton G, and Smith CI (1997). Gap junctions promote the bystander effect of herpes simplex virus thymidine kinase *in vivo*. *Cancer Res* **57,** 1523–1528.
[46] McLaughlin PM, Harmsen MC, Dokter WH, Kroesen BJ, van der Molen H, Brinker MG, Hollema H, Ruiters MH, Buys CH, and de Leij F (2001). The epithelial glycoprotein 2 (EGP-2) promoter-driven epithelial-specific expression of EGP-2 in transgenic mice: a new model to study carcinoma-directed immunotherapy. *Cancer Res* **61,** 4105–4111.